npj | clean water

Perspective

Published in partnership with King Fahd University of Petroleum & Minerals

https://doi.org/10.1038/s41545-024-00345-2

Economic nanobubbles by RFB and promoted PEF with yolk@double-shell structural photocatalyst for degradation of pharmaceutical pollutants

Saeed Shirazian[1,2] ✉, Sameer Alshehri[3], Mohammad A. Khasawneh[4], Masoud Habibi Zare[5] & Arjomand Mehrabani-Zeinabad[5]

In this research, the generation of nanobubbles was carried out using a structure of vortex pump based on the relative blockage of flow (without the use of venturi and orifices, which consume a lot of energy to generate nanobubbles), which has made this process economical and commercial. In addition, the use of advanced synthesized nanoreactors with the Yolk@Shell structure, which forms a photoanode by coating the anode electrode and can operate in the visible light range, has highlighted this research work. An in-depth study of the synergistic effect of advanced photoelectrofenton oxidation methods in addition to the hydrodynamic reactor has shown that the intelligent selection of these three types of advanced oxidation methods together has improved the performance of each other and solved their negative aspects, including the use of hydrogen peroxide, divalent iron ion, and the removal of sludge generated by the electrofenton method. The use of hollow cylindrical electrodes allowed adequate loading of the advanced synthesized nanoreactors with Yolk@Shell structure. The investigation of the effects of micro (advanced synthesized nanoreactors with Yolk@Shell structure) and macro (vortex structure based on relative blockage of the flow) processes on the degradation of pharmaceutical pollutants, both separately and in combination, is a focus of this work. At the end, the energy consumption for each of these processes and this system in general was studied, which showed that the operating cost of this combined system according to the energy consumption requirements for the almost complete removal of the pollutant naproxen and the 90% reduction of its chemical oxygen demand is 6530 Rials/L.h (or 0.15525 USD/L.h), which presents this system as an economical method with industrialization capability. The degradability index (DI) of the introduced system under optimal operating conditions was 3.38, which shows that the development of the system based on the combination of advanced oxidation methods is a suitable method used in this research work due to its environmental friendliness, absence of side effluent production, efficiency and high degradation performance, ability to recover the nanocatalyst and consequently economic efficiency.

In recent decades, various pharmaceutical compounds such as antibiotics, hormones, and tranquilizers have been detected in wastewater from urban wastewater treatment plants (WWTP), in ground and surface waters, and even in drinking water, posing one of the most dangerous health threats to living organisms[1]. Electrochemical advanced oxidation processes have been used in recent years as environmentally friendly technologies and clean processes for the treatment of all types of wastewater[2,3]. Isothermal boiling is a composite phenomenon of formation, growth, and destruction of nano-microbubbles that occurs in short time intervals and consequently releases a lot of energy. Isothermal boiling also leads to the formation of reactive free radicals (hydroxyl), an increase in the solid catalyst level, and an increase in the mass transfer rate due to the turbulence generated in the liquid

A full list of affiliations appears at the end of the paper. ✉e-mail: saeedshirazian@duytan.edu.vn

circulation[4]. Isothermal boiling based on relative flow blockage (RFB) can be replaced by the ultrasonic process (used in the sonoelectrofenton process) as this process is more energy efficient and, more importantly, can be used on a larger scale[5]. The use of advanced oxidation methods in combined form is a suitable solution to improve and increase efficiency compared to using each method separately[6–8]. Numerous research reports have described the degradation of naproxen (NAP) by various hybrid remediation methods based on advanced oxidation techniques[9]. The degradation of naproxen has been studied by various methods, including ultraviolet (UV) radiation (wavelength = 254 nm), vacuum UV (VUV) (wavelength = 172 nm), and the hybrid method of VUV/UV. The results of the experiments show that naproxen is completely degraded after 20 min of UV light, 10 min of UV light or 8 min of UV/VUV light exposure[9,10]. Using the VUV method, a very effective strategy for the mineralization of naproxen was developed, so that after 2 h of irradiation the mineralization of naproxen had almost reached its full potential. It was shown that removal of naproxen by UV/VUV and UV methods resulted in mineralization of 85% and 80% of naproxen after 2 h of irradiation, respectively, with the combined method not necessarily achieving the best mineralization results[10]. the photocatalytic application of UV/TiO_2 to remove naproxen from various aqueous matrices was investigated[11]. The results of the treatment process with the TiO_2 catalyst showed a 19% reduction of dissolved organic carbon (DOC) in the form of a drinking water matrix and a 30% reduction in the distilled water matrix after 3 h of the treatment process[11]. The use of UV/H_2O_2 and UV processes for the removal of pharmaceuticals from WWTP effluent was investigated, including about 10 types of tranquilizers and 12 types of antibiotics[12]. The UV process was found to have a removal efficiency of 90% for the pharmaceuticals present, including naproxen, at a concentration of 923 $\frac{mJ}{cm^2}$. The residual concentration of dissolved organic carbon in the treated wastewater was lower with the combination of UV/H_2O_2 processes than with UV treatment alone, so that more hydroxyl is formed by UV photolysis in terms of direct hydroxyl participation when these processes are combined[12]. The removal of carbamazepine drug was investigated by hybrid purification methods based on hydrodynamic cavitation and H_2O_2 (different molar ratios from 1 to 6) at an inlet pressure (P_{in}) of 4 bar and a pH of 4[13]. In the reported study, carbamazepine removal was enhanced from 31 to less than 58% with an increasing molar ratio from 1 to 5. It was also reported that increasing the molar ratio of H_2O_2 up to 6 showed a reduction in solute degradation rate, which is because of the scavenging of residual H_2O_2 at the highest loading. Above the optimum H_2O_2 loading, the OH radicals formed with H_2O_2 react[9,13]. The photoelectrofenton (PEF) process, as one of the effective combined methods comprising the electrofenton (EF) method together with the use of catalytic materials with Yolk@Shell structure as a nanoreactor, is a promising solution for the removal of pharmaceutical impurities from water. By combining advanced oxidation methods, the weaknesses of the individual methods can be overcome. To this end, in the development of the hybrid photoelectrode clay process, identified as a photochemical process, the intelligent choice of iron as an anode electrode can avoid the addition of divalent iron ions that cause sludge formation in the purification system. Also, the application of the physical method of isothermal boiling based on the relative obstruction of the flow, which is defined as a phenomenon for the disintegration of nano-microbubbles with a high order of released energy, is a worthy choice to replace the chemical substance hydrogen peroxide (H_2O_2) used in the Fenton process, which in addition to the economic savings, introduces the system presents in this research as a green and environmentally friendly process. Evaluation of the recently developed nanocatalysts for energy applications reveals that catalysts with sophisticated structures perform better than the traditional simple catalysts, and catalysts with yolk@shell structure perform the best for catalytic reactions. Developed nanoparticles with Yolk-shell structure or "*nanorattels*" have been prepared and used recently owing to their superior properties and performance in various fields such as catalytic reactors, energy conversion, water treatment, etc. The requirements of catalysts such as high reactivity, long lifetime, selectivity, stability, and reusability are satisfied by using Yolk-shell nanoparticles (YSNs). In this catalytic structure,

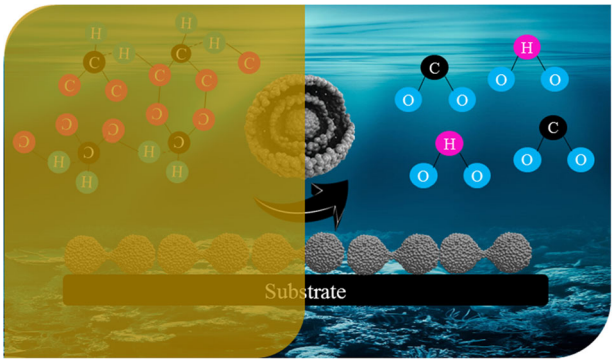

Fig. 1 | Schematic representation of the structure of yolk@shell nanoreactors applied to the anode electrode.

the core is the active site for chemical reactions, while the shells prevent the decay process during the chemical reactions on the surface of the catalyst[14]. The selection of the materials TiO_2, Fe_3O_4, and ZrO_2 in the structural nanoreactor fulfills all the properties mentioned as illustrated in Fig. 1.

One of the most common structural features of the yolk@shell is its ratchet-like structure, the empty space in this structure gives features to this nanoreactor[15,16]. Furthermore, in this design, the YSN shells usually have porous structure which allow diffusion of species into and out of the YSN, while protecting the metal core[15,16]. Also, due to the difference between the chemical and physical characteristics of YSN, several chemical reactions can take place simultaneously over the surface of these materials. Another feature of this structure is that the YSN core surrounded by active sites can move inside the shell, thereby allowing species to reach the catalysts' active sites easily. This property of YSNs is of great importance as it improves the catalytic activity for chemical reactions[15,16]. The free space between the shell and yolk in YSNs offer a homogeneous environment which is suitable for chemical reactions to take place, thus reducing the environmental effects[14–16].

Development and synthesis of porous-based nanomaterials with voids inside a shell has gained momentum recently in various applications such as catalytic reactors, energy storage, and environmental engineering owing to the superior and sophisticated characteristics of these materials like high surface area per unit volume, accessible void space, and adjustable shell-porous configuration[15,16]. One of the disadvantages of the MOF structure is the poor water stability of pure MOFs, as water molecules can attack the coordination bonds between metal ions and organic ligands[17]. Another limitation of the MOF structure is the insolubility, poor processability, and brittleness of pure MOF particles, which limits their application in water purification to remove impurities. In addition, the consumption, loss, and clogging of MOFs in reactor lines and the lengthy and complicated recycling process hinder the widespread use of MOF structures[18–20]. The challenges and limitations of using metal-organic frameworks for wastewater treatment include insolubility, poor processability, brittleness, safety risks, and difficult separation from aqueous solutions[18–20]. Although MOFs possess some advantages, there are also several drawbacks associated with these materials like high cost, poor chemical stability, toxic nature, materials regeneration in the process, efficient isolation of powder, and lack of targeted absorption[21,22].

The use of magnetic iron oxide nanoparticles (Fe_3O_4) as one of the species employed in the yolk@shell materials not only increases the functionality of prepared nanophotocatalyst, but also helps in the recovery and separation of catalyst from mixture in water treatment process[15,16]. Zirconium dioxide (ZrO_2) is recognized as a photocatalyst that has two characteristics owing to its acidic and natural properties: oxidation and reduction. Zirconia is often utilized as a heterogeneous photocatalyst because of its superior characteristics. Due to its relatively large band gap, zirconia (ZrO_2) has been used as the first shell in the yolk@shell materials, in addition to maximizing the use of the properties of this architectural structure, from the rapid recombination of electron-hole pairs generated by

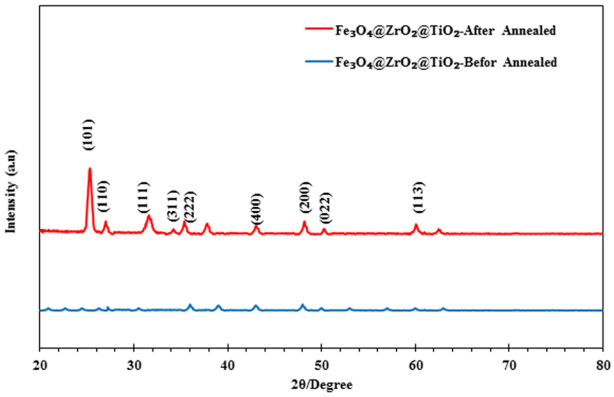

Fig. 2 | X-ray diffraction spectrum of structural nanoparticles with yolk@shell Fe_3O_4@ZrO_2@TiO_2 architecture coated on iron electrode: without heat treatment and after heat treatment (at 550 °C).

the semiconductor material to prevent the second shell as well[15,16]. Titanium dioxide (TiO_2) is one of the most active semiconductor materials utilized in wastewater treatment by photocatalytic-based process. However, it was found that the activity of TiO_2 in photocatalytic reactions is adjustable by tuning several parameters such as material porosity, structural design, electron-hole pair recombination, size of particles, and co-catalysts. TiO_2 was chosen as the second shell in the architectural structure of the yolk@-shell as reported previously[15,16].

This research is generally concerned with the development of the green system based on advanced oxidation-hybrid methods for the degradation of the pharmaceutical pollutant naproxen from the synthetic wastewater, the advanced oxidation PEF hybrid process using the structural Y@DS FZT nanocatalyst[23,24] coating as a thin film coating on the electrode is evaluated, and then the isothermal boiling process based on the RFB is added to this system to generate nano-microbubbles, and the process of degradation and removal of the pharmaceutical pollutant naproxen from the synthesized wastewater solution is evaluated and studied. The main objective of this research is to investigate the performance of intelligently designed nanoreactors with Yolk@Shell structure (Y@DS FZT) coated in the visible light region and in the form of a thin film on the surface of the electrode. The performance of these intelligently designed nanoreactors for the degradation of naproxen together with EF and hydrodynamic reactor processes whose activity is based on isothermal boiling based on RFB, will be evaluated. In short, the main objective of this research is to develop an environmentally friendly system that utilizes the combination of advanced oxidation methods to degrade and remove the pharmaceutical pollutant naproxen from the synthesized wastewater solution.

Result and discussion

Characterization and analysis of electrode coating

Figure 2 first shows the X-ray diffraction spectrum of the structural Fe_3O_4@ZrO_2@TiO_2 nanoparticles with yolk@shell architecture, which were coated on the iron electrode before heat treatment (calcination process). It shows the amorphous phase of the coating to some extent. The X-ray diffraction spectrum shows the layer of Fe_3O_4@ZrO_2@TiO_2 nanoparticles with yolk@shell architecture coated on the iron electrode base after calcination at 550 °C. The obtained peaks demonstrate the coating of the iron electrode with structured nanoparticles. The nanometer size of the particles can be predicted from the appearance of the graph and the width of the peaks.

FESEM images of the surface coating of the anode electrode with yolk@shell Fe_3O_4@ZrO_2@TiO_2 nanoparticles, as shown in Figs. 3a–f and 4a–d, show that the growth process of the nanoparticles on the electrode occurs mainly in layers and partially in the form of an island. As can be seen from the images, the entire surface of the electrode is uniformly and similarly covered with structural nanoparticles with yolk@shell

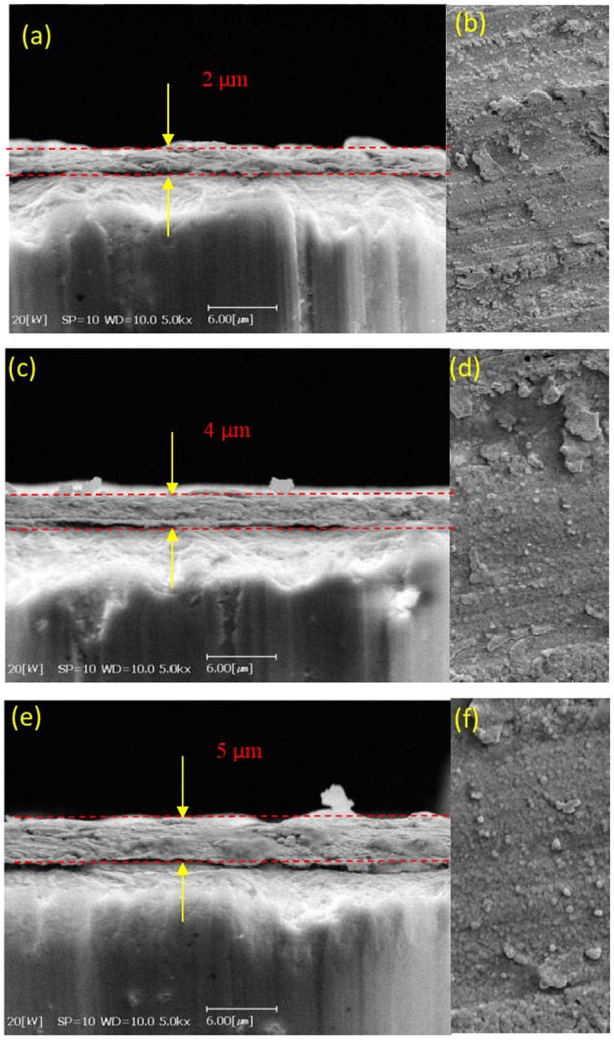

Fig. 3 | SEM images of the coated samples from the surface and in cross-section at each stage. a, **b** The first stage of coating. **c**, **d** The second stage of coating. **e**, **f** The third stage of coating (before the calcination process).

architecture. The thickness of the nanoparticle coating on the surface of the electrode was increased from 2 µm to 5 µm depending on the number of times the electrode was immersed in the nanoparticle suspension solution. The thickness of the nanoparticle coating on the final electrode sample after the calcination process at 550 °C shows a reduction of the coating by 2 µm. According to the results obtained, the number of nanoparticles coated on the electrode surface at each dipping step is about 0.27 g, 1.43 g, and 2.83 g (5.00 g of nanoparticles in each suspension solution), with coating efficiencies of 5.40%, 22.60%, and 23.20%, respectively.

The photoluminescence properties of structural nanoparticles coated on an iron electrode were measured with the PerkinElmer Lambda25 LS5 spectrometer using xenon lamp radiation as an excitation source with a wavelength of 293 nm in the range of 400–700 nm. The photoluminescence spectrum of the thin film coated with Fe_3O_4@ZrO_2@TiO_2 nanoparticles with yolk@shell architecture is shown in Fig. 5. The general aspects of the photoluminescence (PL) spectrum of structural Fe_3O_4@ZrO_2@TiO_2 nanoparticles with yolk@shell architecture can be divided into two categories, including the emission from band edges and the emission from deep levels within the band gap. The width of the band in the visible light region of the spectrum can be justified by dividing it into narrower bands. In addition to relatively weak peaks in the range from 560 to 700 nm, stronger peaks were also detected in the range from 415 to 542 nm. In this range, an intense band with greater sharpness in the visible light region centered at 452 nm, is more prominent than the rest.

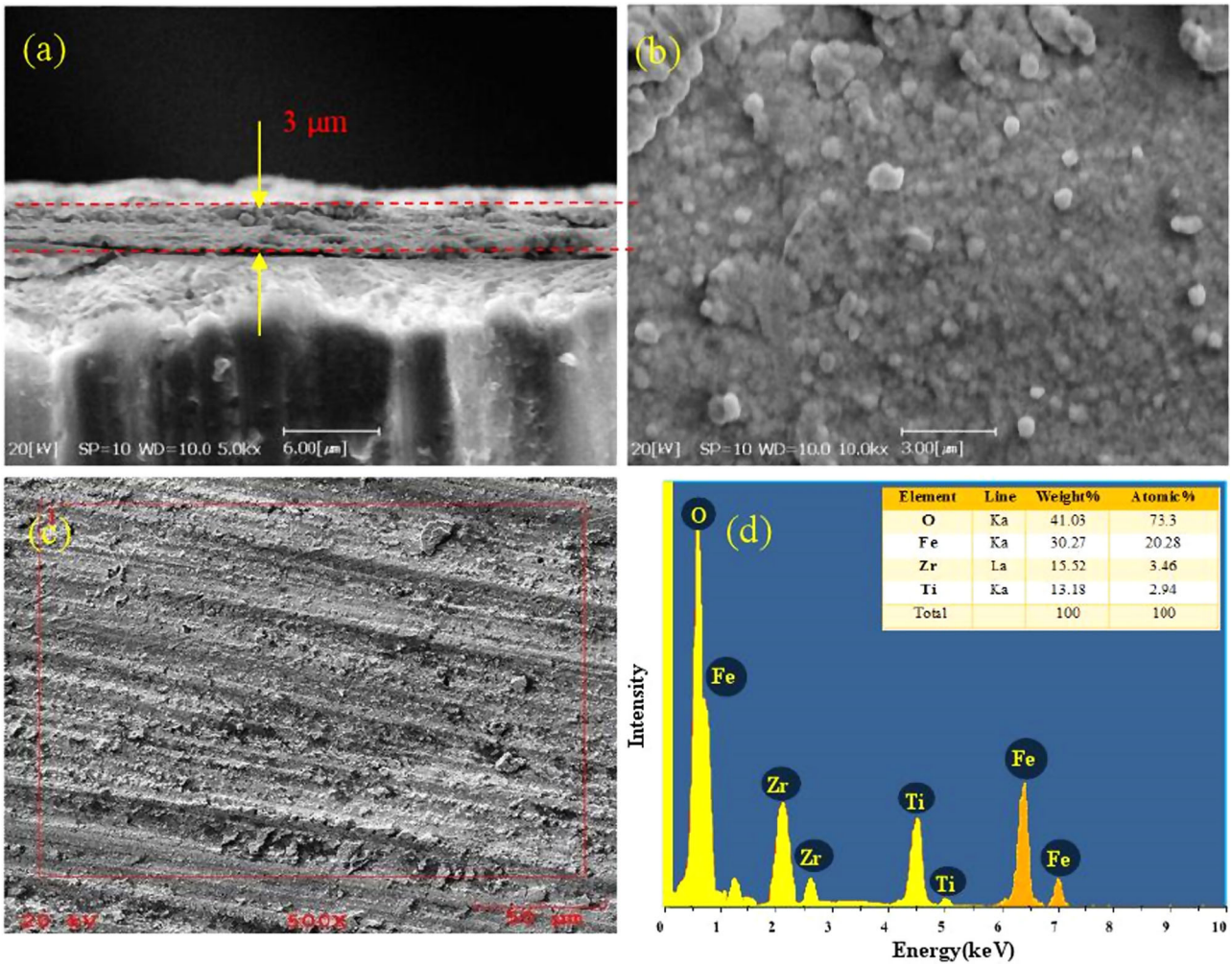

Fig. 4 | SEM images of the coated samples from the surface and in cross-section at each stage. a, **b** The third stage of coating (after the calcination process). **c**, **d** EDS analysis of anode electrode coating.

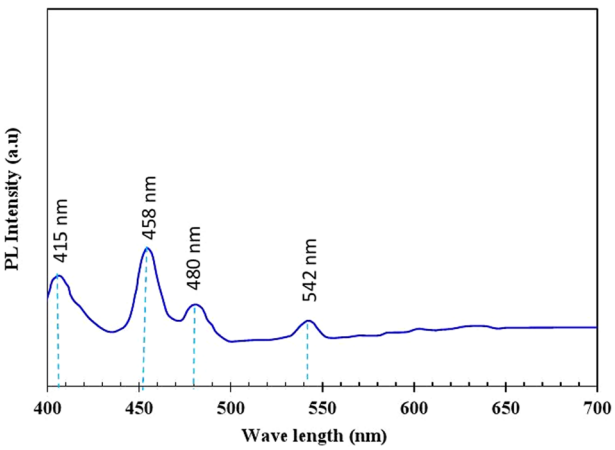

Fig. 5 | Photoluminescence spectrum of patterned nanoparticles with Fe_3O_4@ZrO_2@TiO_2 yolk@shell architecture coated on iron electrode.

Investigating the effect of advanced oxidation hybrid system process characteristics on naproxen removal efficiency

In this section, the effect of the process parameters associated with the hybrid system for advanced oxidation on the extent of naproxen degradation was investigated and evaluated. Initially, the hybrid system started its activity with the isothermal boiling process based on RFB. For this purpose, the optimal conditions of this process including the effects of P_{in}, C_v, pH, and concentration of the pollutant naproxen were determined. Subsequently, the EF process started to operate as the next advanced oxidation process in the system, which was studied and evaluated in conjunction with the RFB process (according to the optimal conditions determined). To continue the photocatalytic activity, structural nanoparticles with yolk@shell architecture were then added to the system and coated on the anode electrode, and the performance of the hybrid system was investigated in degrading the pollutant naproxen. The most important point of the EF process is the removal of hydrogen peroxide and divalent iron ions from the process and its replacement by the RFB process and the iron anode electrode.

The Effect of P_{in} and C_v on the hybrid system for naproxen removal

In the RFB process, the P_{in} and C_v play a very crucial role in determining the intensity of nanobubble production and thus contaminant removal[25]. The effect of P_{in} and C_v on the efficiency of naproxen removal was investigated by changing the P_{in} at a natural solution pH (actual value 7) from 1 to 6 bar. The C_v value is based on the pressure drop between the relative blockage of the channel (in the pump chamber) and the point furthest downstream from the relative blockage of the channel, plus the velocity drop (Kinetic Head) at the relative blockage of the flow, which is considered to be the starting point of the cavitation achieved, was calculated[26]. The calculations for the C_v are shown in Table 1. Normally, cavities are generated at C_v less than 1 ($C_v \leq 1$),

Table 1 | Effect of P_{in} and C_v on naproxen degradation efficiency (NDE) and kinetic rate constants (k_{rc})

P_{in} (bar)	Flowrate (L/h)	Velocity (m/s)	C_v (-)	NDE (%)	k_{rc} (min^{-1})
1	496.96	17.44	0.63	13.88	0.0011
2	646.60	22.69	0.37	18.84	0.0014
3	755.72	26.52	0.27	25.40	0.0021
4	821.65	28.84	0.23	27.38	0.0023
5	858.59	30.13	0.21	26.88	0.0022
6	931.09	32.68	0.18	25.86	0.0022

and the highest activity of cavity generation is achieved in the range of C_v from 0.1 to 0.3[27]. The changes in C_v for different inlet pressures in the range of 1–6 bar are shown in Table 1. The trends show that when the P_{in} is increased from 1 to 6 bar, the C_v decreases from 0.63 to 0.18, which is due to the increase of the volume flow velocity in the whole main line and the increase of the velocity in the relative blockage channel. The results for the degradation amount of the synthetic naproxen effluent in a period of 120 min as the time of the treatment process and the kinetic rate constants (k_{rc}) corresponding to different input pressures (P_{in}) are shown in Fig. 6a, b (under conditions: C_{in} of naproxen 10 mg/L), respectively. The amount of degradation obtained with an increase in the P_{in} from 1 to 4 bar increased with an increase in the P_{in}, and this amount increased with a further increase in P_{in} as well. The highest degradation of 27.38% was obtained at an operating pressure of 4 bar with a C_v of 0.23 ($C_v = 0.23$) and a constant rate of $2.31 \times 10^{-3} min^{-1}$ (Table 1).

At a P_{in} of up to 4 bar, the strong decay of the cavities leads to a higher pressure pulse, which finally breaks the structure of water molecules, causing the formation of hydroxyl[9,28]. The degradation of naproxen is increased when the P_{in} is increased to its optimum value. On the other hand, the lower degradation of naproxen after exceeding the optimal point of P_{in} is due to the lower production of cavity due to the formation of the observed cavity mass[29]. Based on the interpretation of these results, a pressure of 4 bar was chosen as the optimal P_{in} for the next experiments. A comparison of the results obtained in this research work regarding the optimum P_{in} and C_v with the results obtained in other works can be very valuable. The effect of P_{in} and C_v on the degradation of the dye Orange-G was investigated[30]. Their results showed that at a P_{in} of 3 bar, a decolorization of about 92% was achieved using a slotted venturi. In comparison, a lower decolorization rate of 76% and 45% was obtained using a round venturi and an orifice plate under the same conditions as cavity production. The obtained results were very close to reality, as in the slotted venturi there was a relatively higher volume flow at constant pressure drop, a lower C_v, and a higher intensity of cavity production activity showed. The obtained results show that the intensity of cavitation generation ultimately depends on the geometry of the cavitation device. In the present study, isothermal boiling based on relative blockage of the fluid channel in the two-phase pump structure was used as the equipment for cavity production, and this choice was confirmed by the reported results. The effect of P_{in} (3–10 bar) on the treatment process of textile dyeing wastewater via a slotted venturi was investigated and reported previously[31]. A decrease in total organic carbon (TOC) and COD was observed when the P_{in} was increased by a factor of 3 to 5. At an optimal value of P_{in} which is 5 bar (optimum $C_v = 0.07$) and a duration of 120 min, the largest reduction in TOC and COD and color is 12% and 17%, and 25%, respectively, while the reduction in COD and lower TOC at a P_{in} of 10 bar is as high as 3.5% and 9.3%. A maximum contaminant removal of 4-nitrophenol of 12% was reported at an optimum P_{in} of 5 bar using a venturi as a cavity production unit[32], while Raut Jadhav et al. reported a maximum contaminant removal of 6-chloro-3-pyridylmethyl of 26.5% at an optimum P_{in} of 15 bar[10]. In the present study, the maximum amount of naproxen degradation was obtained by relatively blocking the fluid channel in the two-phase pump structure as a cavity production device at an optimal P_{in} of 4 bar. The difference in the presented research proves that the optimal value of the P_{in} depends on the type of wastewater or target pollutants, thus confirming the ongoing research to prove the existence of an optimal P_{in}[9].

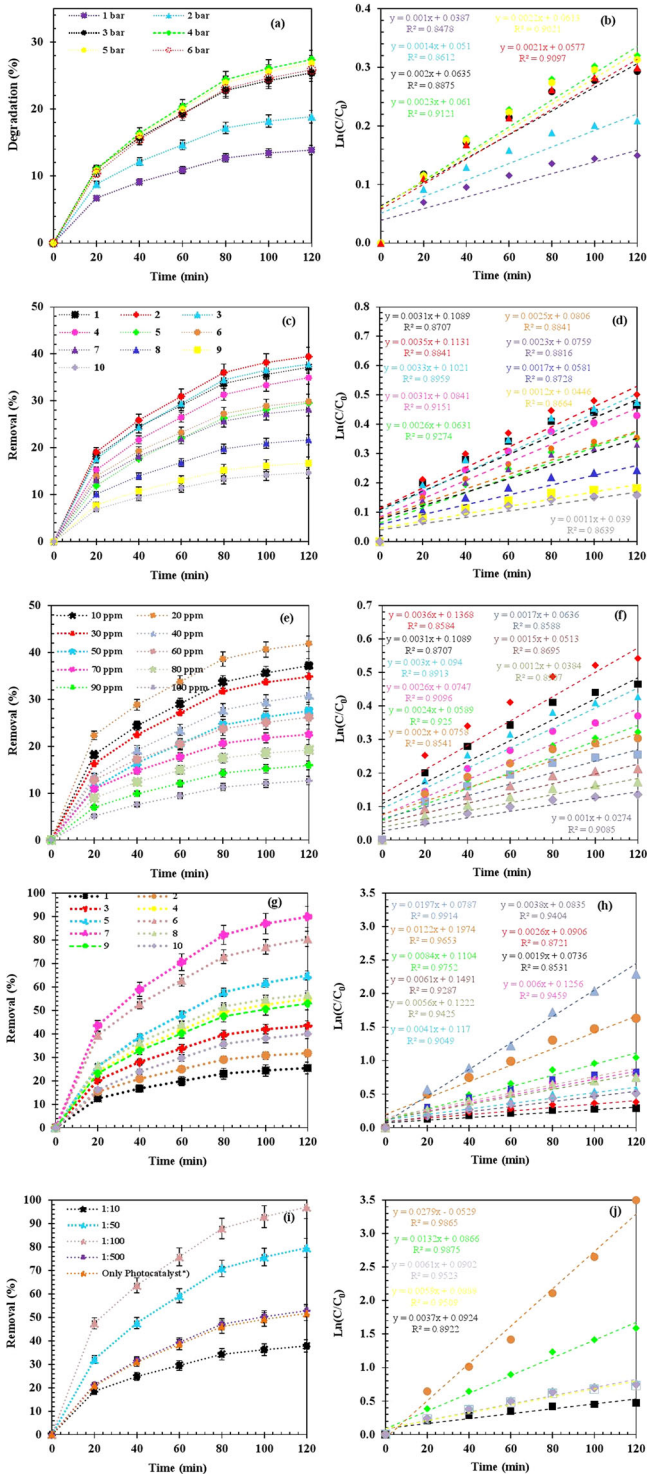

Fig. 6 | Effect of process parameters on the NPX removal and removal kinetics data. Effect of **a** P_{in} on NDE, **b** fitting kinetic data at different inlet pressures (P_{in}), effect of **c** pH on NDE, **d** fit of kinetic data at different pH values, effect of **e** C_{in} on NDE (using the RFB method), **f** fit of kinetic data at different inlet concentrations (C_{in}), effect of **g** voltage on NDE (along with the EF process), **h** fitting kinetic data at different voltages, **i** effect of combined RFB and PEF process on NDE, **j** fitting of kinetic data (NPX: P as 1000)*.

The Effect of pH on the hybrid system for the removal of naproxen

The pH of the operating environment can vary the chemical characteristics of solution and the pollutant environment and finally has a significant effect on the improvement of the degradation process[33]. In this research, a series of

Table 2 | Effect of pH on NDE and k_{rc}

pH	NDE (%)	k_{rc} (min^{-1})
1	37.15	0.00311
2	39.43	0.00352
3	37.80	0.00331
4	34.94	0.00312
5	29.57	0.00263
6	29.88	0.00254
7	28.18	0.00236
8	21.68	0.00175
9	16.71	0.00129
10	14.67	0.00116

experiments were conducted in the pH range from 1 to 10 to investigate and verify the effect of pH on the optimized P_{in} four times. The results obtained from the investigation of the effects of pH on the degradability of naproxen are shown in Fig. 6c, d (under conditions of a P_{in} of 4 bar and a naproxen concentration of 10 mg/L), while the ultimate degradability and kinetic degradation k_{rc} are given in Table 2.

The highest NDE was 39.43% and the decrease in COD was 11.30% with a k_{rc} of $3.52 \times 10^{-3}\,min^{-1}$ at pH=2. Under alkaline conditions (pH = 10), an NDE of 14.67% was determined with a lowest k_{rc} of $1.16 \times 10^{-3}\,min^{-1}$. The NDE and k_{rc} were higher under acidic conditions than under alkaline conditions, which is due to the fact that the oxidation potential of hydroxyl under acidic conditions is high and the rate of hydroxyl recombination is low[26,34]. The effect of the pH value of the solution on the decolorization process was investigated by changing the pH value (range 2–10) five times at constant pressure[35]. According to the results, the decolorization rate is more at the acidic environment compared to the basic one. Indeed, the highest decolorization rate of 32.32% was reported with a k_{rc} of $3.41 \times 10^{-3}\,min^{-1}$ at pH = 2, while the degradation rate of decolorization at pH = 10 was 3.89%. It has been recognized that acidic environment is suitable for the degradation of pollutant atrazine[36]. The determined k_{rc} for atrazine degradation was reduced from $1.50 \times 10^{-3}\,min^{-1}$ to $5 \times 10^{-3}\,min^{-1}$ by enhancing pH value from 3 to 7.3. The degradation of Red-120 dye by hydrodynamic cavitation was studied and reported that the decolorization was about 60% and the TOC reduction was 28% during the three-hour treatment process at pH = 2[33]. It is of great importance to point out that several works have reported that pH has little influence on the pollutant degradation rate in the treatment process. For complying with the principles of final discharge, the pH of the wastewater must be readjusted after the treatment process, so pH adjustment cannot always be suggested and depends on each scenario[9]. Under the optimal process conditions used, a pH of 2 resulted in a significant increase in the NDE, so a pH of 2 was chosen as optimal for the next experiments.

The effect of the C_{in} of naproxen on the hybrid system of naproxen removal

The degradation of naproxen in different C_{in} of this pollutant, ranging from 10 to 100 mg/L, was studied using the RFB method at an optimal P_{in} of 4 bar and an optimal pH of 2. The obtained results, including the efficiency of naproxen degradation and the k_{rc}, were presented in Table 3, while the information related to the change of the degradation value and the k_{rc} of the degradation process were shown in Fig. 6e, f (under conditions: P_{in} 4 bar, pH of naproxen feed solution equal to 2).

The efficiency of naproxen degradation increased from 12.67 to 37.16% when the C_{in} was decreased from 100 to 20 mg/L. At a C_{in} of 20 mg/L naproxen with a k_{rc} of $3.67 \times 10^{-3}\,min^{-1}$, the highest degradation of 41.84% was achieved, while at a C_{in} of 100 mg/L naproxen with a k_{rc} of $1.08 \times 10^{-3}\,min^{-1}$, only 12.67% degradation was achieved (Fig. 6e, f). Based on the results obtained, it can be argued that as the C_{in} increases, the amount of pollutant molecules increases, while the hydroxyl radicals

Table 3 | The effect of C_{in} on NDE and k_{rc}

C_{in} (mg/L)	NDE (%)	k_{rc} (min^{-1})
10	37.16	0.00318
20	41.84	0.00367
30	34.80	0.00309
40	30.92	0.00263
50	27.52	0.00242
60	26.16	0.00209
70	22.51	0.00171
80	19.17	0.00156
90	15.91	0.00126
10	12.67	0.00108

Table 4 | effect of C_{in} on NDE and k_{rc} in the combined process of RFB and EF

Voltage (V)	NDE (%)	k_{rc} (min^{-1})
1	25.44	0.00065
2	31.76	0.00195
3	43.42	0.00385
4	54.95	0.00563
5	64.90	0.00842
6	80.47	0.01221
7	89.91	0.01972
8	56.67	0.00612
9	52.92	0.00415
10	40.03	0.00265

produced remain constant[37]. A similar trend of decreasing the degree of destruction with increasing C_{in} was found already for the pollutant potassium ferrocyanide between 20 and 200 mg/L[38]. At a C_{in} of 20 mg/L of potassium ferrocyanide, the highest degradation was achieved at 20.76%, while at a C_{in} of 200 mg/L and a constant energy input (power) in 0.1 L, only 8.02% degradation was achieved[9,26]. In view of the fact that in the research work the highest value of NDE was achieved at a C_{in} of 20 mg/L of the pollutant, the remaining experiments were carried out with a C_{in} of 20 mg/L as the C_{in} of naproxen.

In this phase of the experiments related to the development of the hybrid system, the conditions of the RFB process were optimized, and in the continuation of the EF process, two electrodes, anode (iron) and cathode (graphite), were added to the system in the form of a hollow cylinder and coaxial (see Supplementary Information). The distance between the electrodes was considered constant.

The effect of the voltage of the EF process on the hybrid system for the removal of naproxen

The naproxen degradation process by a hybrid system comprising the EF process under different voltages from 1 to 10 volts and the RFB process was investigated and evaluated under optimal P_{in} conditions of 4 and pH = 2 and a C_{in} of 20 mg/L. The results obtained, including the percentage of naproxen degradation and the k_{rc}, are shown in Table 4, while the corresponding graph of the amount and kinetic constant of degradation is shown in Fig. 6g, h (under conditions: P_{in} 4 bar, feed solution pH 2, naproxen concentration 20 mg/L).

Looking at the effect of the RFB process, as the voltage of the EF process increased from 1 to 7 V, the NDE increased from 25.44% to 89.91%, then during a downward trend, the NDE decreased to 40.03% due to the increase in voltage from 8 to 10 V. At an operating voltage of 7 V, the highest degradation of naproxen was 89.91%, and the k_{rc} was calculated to be

Table 5 | Effect of catalyst loading on NDE and k_{rc} in the combined RFB and PEF treatment process

NAP/Catalyst	NDE (%)	k_{rc} (min^{-1})
1:10	37.78	0.00375
1:50	79.58	0.01322
1:100	98.97	0.02791
1:500	52.85	0.00618
Catalyst alone (1:100 ratio of NAP:Catalyst)	51.68	0.00595

$1.972 \times 10^{-2}\,min^{-1}$ under these conditions, while at a voltage of 1 V, the NDE was 25.44% and the k_{rc} was $6.5 \times 10^{-4}\,min^{-1}$ (Fig. 6h).

Based on the results obtained, it can be argued that increasing the voltage up to the optimal voltage value of 7 V leads to an increase in hydroxyl production and increases the overall efficiency, resulting in an increase in the efficiency of naproxen degradation[37]. As the voltage increased further, a bubble film formed on the electrodes, as shown in Supplementary Information. The occurrence of this phenomenon had a detrimental effect on hydroxyl production, decreasing the overall process efficiency. According to the results obtained, the positive effect of adding the EF process to the hybrid system was observed. As known, the degradation of naproxen was increased by 48.07% in the best case of the process. In other words, the efficiency of the hybrid system increased by 114.89%. In view of the fact that in the present study the maximum degradation performance was achieved at an applied voltage of 7 V, the other experiments were carried out with an applied voltage of 7 V as the optimum voltage.

Effect of the photocatalyst with Fe_3O_4@ZrO_2@TiO_2 Yolk@Shell structure on the hybrid system for the removal of naproxen

The developed combined RFB and PEF system was used to degrade naproxen at different loadings of photocatalyst (P) using different mass ratios of naproxen to photocatalyst (P) in the PEF process (see Table 5). The results obtained are shown in Table 5 and Fig. 6i, j (under conditions: P_{in} 4 bar, pH of feed solution 2, naproxen concentration 20 mg/L, voltage 7 V).

It is noteworthy that the results obtained show an increase in NDE from 37.78% to 98.97% when the ratio of catalyst (P) to naproxen is increased from 10 to 100, while the next increase to 500 leads to a decrease in destruction efficiency by 51.68%. The pseudo-first- order kinetic model is suitable for the removal of naproxen using combined RFB and PEF treatment methods. The maximum NDE was 98.97% and the k_{rc} was $27.91 \times 10^{-3}\,min^{-1}$ at a catalyst (P) to naproxen mass ratio of 100. At the same catalyst (P) to naproxen mass ratio of 100, a maximum reduction in COD of 90% was achieved, which was found to be the optimum value. By using the mass loading of catalyst (P) more than the optimal value, the amount of naproxen degradation was lower due to the scavenging activity (or electron-hole pair formation) of the loaded catalyst (P) residue. NDE and k_{rc} using catalyst (P) (with a molar ratio of 100 to 1) along with the EF process were 51.68% and $5.95 \times 10^{-3}\,min^{-1}$, respectively, proving the role of the EF process in the amount of degradation[9]. In the current research work, it was observed that the pH value has no significant effect on the combined purification method of RFB and PEF in the optimal mass ratio of catalyst (P) loaded to naproxen equal to 100. Naproxen removal efficiency without any adjustment of solution pH for combined P treatment method with RFB process is 86.40%.

Based on the k_{rc}, the efficiency of the RFB and PEF hybrid system was calculated separately for each of the processes using the synergistic index, which is shown below. According to Eq. 1, the synergetic index (f) is calculated on the basis of k_{rc}:

$$f = \left[k_{FRB+PEF}\right] / \left[k_{FRB}\right] + \left[k_{PEF}\right] = \left[27/91 \times 10^{-3}\right] / \left[2/3 \times 10^{-3}\right] + \left[5/95 \times 10^{-3}\right] = 3/38 \quad (1)$$

The synergetic index expresses the greater effect of using the developed combined purification method based on RFB and PEF treatment methods

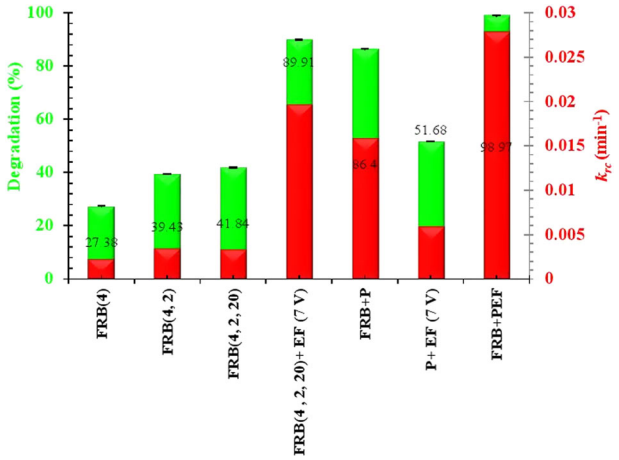

Fig. 7 | Comparison of the results of the synergistic effect obtained by different advanced oxidation methods used in this study to remove naproxen from synthetic wastewater [RFB (P_{in}, pH, concentration)].

Table 6 | Comparison of the results of the synergistic effect obtained by using different advanced oxidation methods

Process	NDE (%)	k_{rc} (min^{-1})
RFB (P = 4 bar)	27.38	0.0023
RFB (P = 4 bar and pH = 2)	39.43	0.00352
RFB (P = 4 bar, pH = 2 and $C_{initial}$ = 20 mg/L)	41.84	0.00367
RFB (P = 4 bar, pH = 2 and $C_{initial}$ = 20 mg/L) +EF (Vol = 7 V)	89.91	0.01972
RFB+Catalyst alone (1:100 ratio of NAP to Catalyst)	86.40	0.01593
EF (Vol = 7 V) +Catalyst alone (1:100 ratio of NAP to Catalyst)	51.68	0.00595
RFB (P = 4 bar, pH = 2 and $C_{initial}$ = 20 mg/L) +EF (Vol = 7 V) +P	98.97	0.02791

than any of the individual treatment methods under the same conditions. The generation of nanobubbles based on isothermal boiling based on RFB leads to local turbulence, which by removing the mass transfer resistance, the PEF process works more effectively and also increases the production of hydroxyl, which ultimately results in the NDE increases the pollutant. From the comparison with the studies and research, it was found that although the process for the loading effect of the catalyst (P) is similar, but the actual optimum value obtained for each pollutant is different, which clearly proves the importance of the present work. The difference in increasing the catalyst dose by adding an external oxidant (catalyst (P)) usually depends on the type of pollutant structure and its reactivity with hydroxyl. Therefore, it is suggested to determine the optimal dose of the catalyst (P) based on the experiment.

The combined system including RFB and PEF process can increase the NDE because of greater production of hydroxyl based on higher mass transfer and triple oxidation mechanisms of direct attack of hydroxyl formed by RFB, catalyst (P) and to improve the driving force resulting from the direct attack of EF and the disturbance and turbulence of the flow resulting from RFB, which results in the reduction of mass transfer resistance[26]. The combination approach of RFB and PEF was studied under the optimal flow rate of 821.65 L/h inside the reaction reactor containing Naproxen aqueous solution, which was previously optimized at pH = 2. Approximate full NDE and 90.00% reduction of COD load with a k_{rc} of $27.91 \times 10^{-3}\,min^{-1}$ using the combined system resulting from the RFB process and PEF according to the information shown in Fig. 7 and Table 6 was obtained.

The system developed using the combination of advanced oxidation processes presents the degradation value of 98.97% of feed as a confirmation

Table 7 | Electricity consumption costs for the different cleaning processes studied in this research

Process Type	NDE (%)	Energy Consumption (kWh)	Total Cost Related to Power Consumption (Rials/L.h)	Total Cost Related to Power Consumption (USD/L.h)[a]
RFB	41.84	0.450	4500	0.10698795
RFB + P	86.40	0.453	4530	0.107701203
RFB + EF	89.91	0.650	6500	0.15453815
RFB + PEF	98.97	0.653	6530	0.155251403

[a]1 IRR = 0.0000237751 USD- (Based on data: Central Bank of the Islamic Republic of Iran- Conversion from US Dollar to Iranian Rial—Last updated on May 4, 2024, 07:53 UTC)

Table 8 | Intensity parameters of combined system processes from an engineering perspective

Process Type	VEI (kJ/L)	SEI (kJ/mmol of Naproxen)	SV (Flow L/min Divided by Volume of Reactor L)
RFB	810	3.24	6.84
RFB + P	815.4	3.2616	
RFB + EF	1170	4.68	
RFB + PEF	1175.4	4.7016	

of a suitable process and presents the synergistic effect of these processes in the best way. This hybrid system reduces mass transfer resistance for all modes and improves the amount of hydroxyl. It should be pointed out that the mass ratios of catalyst to contaminant have been used differently in various research. Therefore, the precise effect of PEF in reducing the concentration of naproxen or COD had not been tested and investigated.

Although the reports of the previous research and the observed trend of the present research work clearly indicate the high and impressive efficiency of the combined method of RFB and PEF compared to each of these treatment methods under investigation in this research alone.

Operation cost of the developed hybrid system treatment process

In order to calculate the operation cost of each of the processes of the hybrid system, the power consumption of that process should be calculated first, and then based on the power consumption rate of the Isfahan electricity dispatching network, this value should be calculated. This operation's cost is calculated only based on the energy consumption rate and its fixed costs are not taken into account. In the reactive reactor including the nanobubble production process based on RFB, the two-phase pump is the main source of energy consumption for nanobubble production. The power consumed by the pump was 450 watts based on the flow rate. Also, in the case of the EF process, the electricity consumption is about 200 watts. Operating cost for various remediation methods was estimated according to power requirements to reduce 90.00% of COD load of wastewater. The obtained information is given in Table 7. The energy consumption costs of the hybrid system presented in this research work have an error budget of 0.1%.

In order to investigate the intensity of the process from a technical point of view, the parameters volumetric energy input (kJ/L), specific energy input(SEI) (kJ/mmol naproxen), and space velocity (flow rate L/min divided by the reactor volume L) were calculated for all processes of the combined system, the results of which are shown in Table 8.

The obtained costs are only shown as an index and cannot be compared for different processes because the amount of naproxen removal and the efficiency of the process are different in each process. The best RFB + PEF treatment requires a treatment cost of only 6530 Rials/L.h (or 0.15525 USD/L.h) while RFB plus EF treatment requires 6500 Rs/L.h (or 0.15454 USD/L.h) based on power requirements. According to Table 9, the results obtained from the degree of degradation of the structure of pharmaceutical pollutants in similar works show the effectiveness of the presented hybrid system[13,39–41].

Methods

Equipment and characterization experimental

X-ray diffraction (XRD) patterns were collected with a Rigaku Ultima IV XRD via a Co-Kα X-ray tube with an input voltage of 40 kV at a 2θ value of 20° to 80° and a scan speed of 1° per min and a 2θ spacing of 0.05°. The crystal details of samples were evaluated using the JCPDS resource. FE-SEM TESCAN MIRA3 was utilized to obtain SEM analyses of samples, to study the morphology of the synthesized nanocatalyst samples, and for EDS analysis to determine the weight and atomic content of the sample elements. With this instrument, surfaces can be photographed with a magnification of 100 to 200,000 times and a resolution of less than 1–20 nm. The determination of the photoluminescence properties of the samples in terms of emission intensity at various wavelengths after their excitation with photons of a specific wavelength was performed by PL analysis or photoluminescence spectroscopy (VARIAN/ECLIPSE CARY)[15,16]. The characteristics of two iron anodes and graphite cathodes manufactured by Azar Electrode Company and used for the naproxen removal process are shown in Supplementary Information. The visible light source (wavelength 400–700 nm) and hydrodynamic reactor used in the system of this research are shown in Supplementary Information.

Hybrid laboratory system method with PEF and isothermal boiling based on RFB

The hybrid process of the developed system was tested in individual steps. As the first process of the combined system, the performance of the RFB-based isothermal boiling process was evaluated based on the optimal parameters, then the effect of the modified EF process was evaluated as the second process of the combined system, and finally, the performance of structural nanoparticles to remove the synthesis wastewater naproxen in the form of a thin layer film coated on an iron electrode was comprehensively evaluated and studied together with the EF process and nanobubble injection based on the RFB-based isothermal boiling.

In most studies on hydrodynamic cavitation, the P_{in} is considered the main parameter. The reason for this is the ease of measurement and control of this parameter rather than its physical significance to the process. A parameter that describes the different states of cavitation (including the start and end points of cavitation and supercavitation) is called the cavitation number, which is defined as follows (based on Eq. (2))[42]:

$$C_v = \frac{P_2 - P_v}{\rho \frac{V_0^2}{2}} \quad (2)$$

where C_v is the cavitation number, P_2 is the recovered downstream pressure, P_v is the water vapor pressure, ρ is the water density, and V_0 is the fluid velocity. Cavitation occurs when the value of C_v is close to or less than the value of C_v (generally $C_v < 3$). Cavitation increases when the C_v value is reduced by decreasing the static pressure or increasing the flow rate.

Treatment process with nanobubble production based on RFB

Although ultrasonic reactors are specifically recommended for high intensity destruction, their operating conditions on a commercial scale are difficult due to the high energy requirements and associated higher costs of the treatment process. Therefore, the RFB-based process for nanobubble production is proposed as an alternative with favorable energy efficiency and

Table 9 | Research on pharmaceutical wastewater treatment using the combined process of cavitation and advanced oxidation

Cavitation Method Combined with						
Type of Pharmaceutical Pollution	**AOP Method**	**$P_{optimal}$ (bar)**	**pH**	**Time (min)**	**Degradation (%)**	**Ref.**
Carbamazepine	-	4	4	120	38.7	13
	$H_2O_2 + O_3$				100	
	O_3				94.4	
	H_2O_2				58.3	
	UV				52.9	
Tetracycline	-	3.4	5.2	90	12.2	39
	TiO_2				78.2	
Pefloxacin	-	-	3.3	120	84.9	40
			5.3		35.5	
	H_2O_2	3	5.3		69.7	
	O_3		-	20	91.5	
Tetracycline	-	-	-	90	33.9	42
	$(TiO_2/Er_3^+:YAlO_3)/NiFe_2O_4)$				84.45	
	TiO_2				59.16	
	$NiFe_2O_4$				52.21	
Naproxen	-	4	2	120	41.84	Present Work
	EF				89.10	
	$Fe_3O_4@ZrO_2@TiO_2 + EF$				98.97	

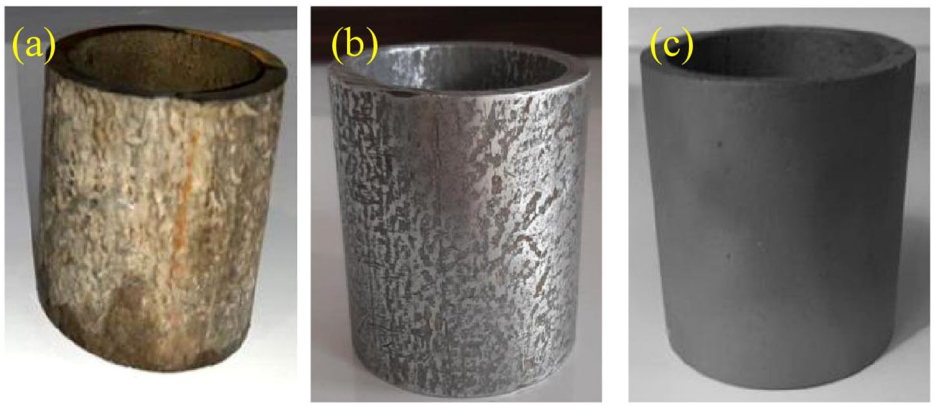

Fig. 8 | Coating steps of the iron electrode sample. **a** Before surface modification, **b** sandblasted, **c** coated and annealed.

good potential for capacity expansion. In order to reduce the cost of the purification process, all experiments were carried out with a hydrodynamic reactor based on the RFB method.

Since the two-phase vortex pump used in this research work generates nanobubbles in the process by partially blocking the flow, the term RFB process is used in the following. In this part of the research work, the effects of operating parameters such as P_{in} (in the limit range of 1–6 bar), pH value (in the range of 1–10) and the initial concentration (C_{in}) of naproxen (10–100 mg/L) were first investigated and studied.

For each test, 2 liters of an aqueous solution with a concentration of 10 mg/L of naproxen and a purification time of 120 min were used. For the combined RFB and catalyst (P) method, different mass ratios of naproxen to catalyst (P) were used, including 1–10, 1–50, 1–100, and 1–500, to investigate the effect of catalyst loading as an oxidizing agent. To analyze the progress of the purification process, samples are taken for analysis at certain time intervals or at the desired end time of the purification process. All treatment experiments were carried out in triplicate to demonstrate reproducibility. According to the report, the average error values of the experiments were given as ±2%. In this hybrid method, an anode electrode with three layers of structural $Fe_3O_4@ZrO_2@TiO_2$ nanoparticles was used.

Preparation and coating of nanoparticles on anode electrode

A hollow cylindrical iron electrode was prepared to coat the surface with nanoparticles. This sample has an effective area of 243 cm^2. First, the surface of the iron electrode was polished with hard sandpaper and then soft sandpaper for 30 min and prepared for coating (see Fig. 8a). Then, the surface of the cylindrical iron electrode was washed with acetone, ethanol and deionized water to remove dust, grease and oil before coating (Fig. 8b). The anode electrode as a support was prepared in a 10% oxalic acid solution for 60 min and dried at 100 °C for 15 min. The suspension solution of architectural nanoparticles with yolk@shell structure $Fe_3O_4@ZrO_2@TiO_2$ (a dark brown solution) was prepared in 150 mL ethanol and dispersed for 30 min using an ultrasonic device. The uniformity of the solution is one of the most important parameters to achieve a uniform coating. The suspension solution of nanoparticles was applied to the iron substrate using the deep immersion method. This material was dried at 100 °C for 30 min and annealed in an oven at 550 °C for 2 h during a specific temperature cycle to cover the first layer. The coating process was repeated three times.

After applying the next layer, the materials were annealed at 550 °C for 2 h as shown in Fig. 8c. To determine the coating, the control sample was subjected to XRD, photoluminescence and SEM analysis.

Table 10 | Technical data of the nanobubble fabrication system

Technical Specifications	Type/Amount	Technical Specifications	Type/Amount
Bubble production process	Two-phase vortex pump	Seal type	Wyton
Pump Model	MOTOGEN-CR71_2B	Reactor Dimensions	15 × 15 × 15 cm
Feeding System	Single phase/50 Hz	Type of Reactor	Plexiglass
Power Consumption	0.55 kW (Nominal)	Reactor Shape	Cube
Maximum Flow Rate	1 m^3/h	Input Connection	3/4“
Vortex Pump Rate	3000 rpm	Output Connection	1/2“
Vortex pump Material	Steele 304–316	Pump Outlet Connection	3/8“

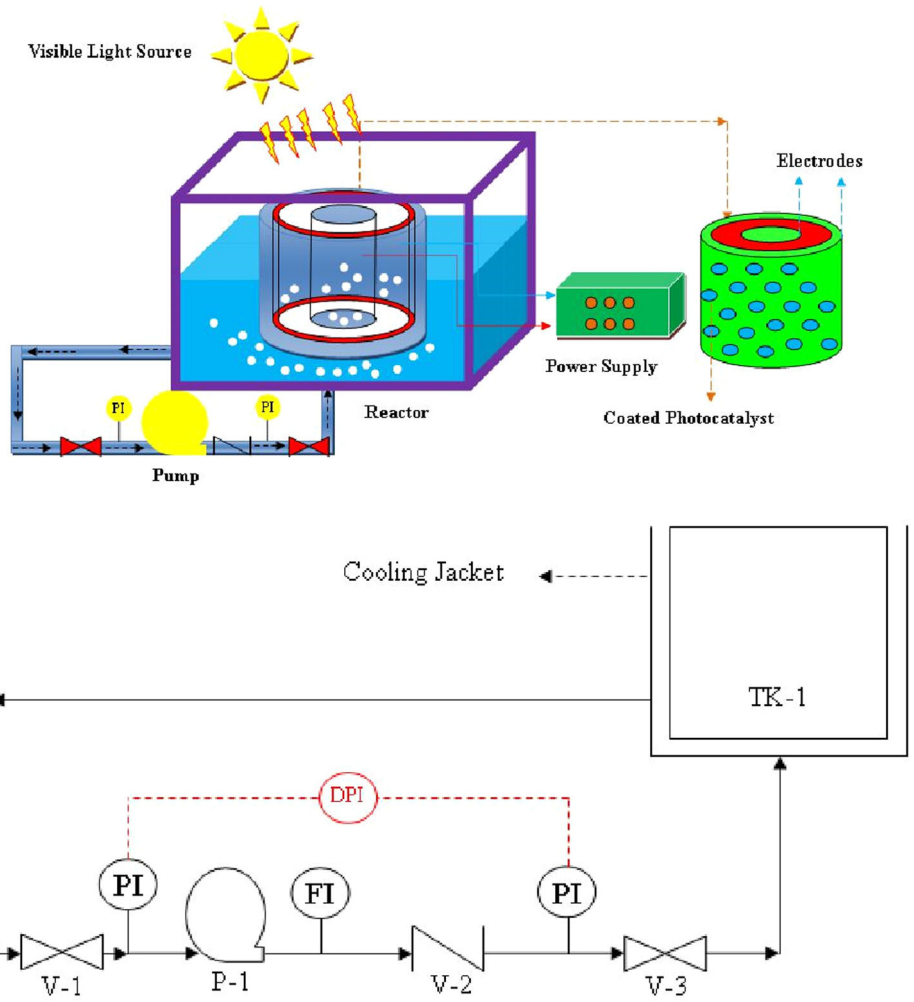

Fig. 9 | Schematic (top) and piping and instrument diagram (bottom) of the PEF system with isothermal boiling based on RFB.

Technical specifications of the hybrid system

To achieve the objectives of this research, a device that has been used in studies related to hydrodynamic reactors for the production of nanobubbles based on a Venturi tube on a laboratory scale was used. The general specifications of the nanobubble production system and the reactive reactor are shown in Table 10.

The configuration of the reactor for the RFB process is shown in Fig. 9. The prepared laboratory system includes a reactor with wastewater, a two-phase vortex pump with a nominal power of 0.55 kW, various control valves and flanges to maintain the device for generating cavities (bubbles). The circulation circuit includes the main pipes, and there is no need for recirculation to effectively control the flow of solution through the bubble production device. The geometric components of the two-phase vortex pump used in the bubble generation device are shown in Table 10 and Fig. 9. The two-phase vortex pump (model CR71_2B) in the reactor configuration for the RFB process was purchased from a specialized water process supplier.

The current system consists of a closed fluid circuit that includes a reaction reactor, a two-phase vortex pump, control valves, piping and connections, service bases, and service flanges. The suction part of the pump is connected to the side of the reactor. In view of the low flow rate (certain parameters in the design) and the need to generate high velocities (generation of a high head by the pump), pump is required that can fulfil these two characteristics - very low flow rate and high head - together.

Development of PEF system with isothermal boiling based on RFB

In this part of the work, the coating of structural nanoparticles with yolk@shell architecture on the electrode is first described and analyzed.

Then, other advanced oxidation processes such as isothermal boiling and EF are added to the system. First, the parameters of the isothermal boiling process were optimized step by step, and finally, the EF process was added to include the hybrid system and the effects of the process parameters of the aforementioned system were investigated.

Analysis of synthesized naproxen effluent with HPLC instrument

The degradation of naproxen was measured with the U-HPLC device from Thermofisher (model 3000 -Ultimate). The mobile phase of acetonitrile and deionized water at a ratio of 60:40 was used as a carrier for the separation under reversed phase conditions (at a rate of 0.8 mL/min). Naproxen concentrations were measured at a wavelength of 210 nm, which was used to detect naproxen concentrations. The slope and standard deviation of the calibration curve were used to determine the limit of quantification (LOQ) and limit of detection (LOD). In the calibration curve for naproxen, the LOD and LOQ were estimated to be 0.21 and 0.07 mg/L, respectively, which is acceptable. All purification samples were analyzed using the same HPLC method to determine the characteristics, and the concentrations were determined using calibration curves. The analysis of the chemical oxygen demand (COD) was carried out with a COD digester provided by the Hana Equipment Company. COD reduction was performed according to the ISO 6060:1989 standard (Water Quality-Determination of COD). Sample vials or glass samples containing wastewater were treated in the COD digester with the reagent's sulfuric acid and potassium dichromate at a temperature of 150 °C and for 2 h. The calibration curve for COD analysis was established using a standard solution (see SIF for more details).

An in-depth study of the synergistic effect of advanced photoelectrofenton oxidation methods together with the injection of economic nanobubbles using a vortex pump structure based on relative blockage of the flow shows the intelligent choice of these three types of advanced oxidation methods together, which improves the degradability index equal to 3.38, and the problems of each of these methods, such as the use of venturi and orifice, which consume a lot of energy to produce nanobubbles, the use of hydrogen peroxide, the presence of divalent iron ions, and the production of sludge by the electrofenton method, have been solved. This combined system with the presence of advanced synthesized nanoreactors with the Yolk@Shell structure, which by covering the anode electrode allows the formation of a photoanode that can operate in the visible light range, provides a strategic perspective in the field of non-biodegradable wastewater treatment. The economic feasibility of this combined system presented also shows the low operating cost of 6530 Rial/L.h (or 0.15525 USD/L.h) for the treatment of each liter of non-biodegradable wastewater and the reduction of the chemical oxygen demand of this wastewater by 90%.

Supplementary material

Specifications and detailed information about the combined system, the electrodes, the electrofenton process, the hydrodynamic reactor, the two-phase pump, the exact measurement method of the COD samples, the calculations of the process parameters, and the calculation of the energy consumption of the green system are included in the supplementary information file.

Data availability

The data supporting this study are available when reasonably requested from the corresponding author.

Received: 12 February 2024; Accepted: 3 June 2024;
Published online: 14 June 2024

References

1. Evgenidou, E. N., Konstantinou, I. K. & Lambropoulou, D. A. Occurrence and removal of transformation products of PPCPs and illicit drugs in wastewaters: a review. *Sci. Total Environ.* **505**, 905–926 (2015).
2. Anotai, J., Lu, M.-C. & Chewpreecha, P. Kinetics of aniline degradation by Fenton and electro-Fenton processes. *Water Res.* **40**, 1841–1847 (2006).
3. Panizza, M. & Cerisola, G. Removal of organic pollutants from industrial wastewater by electrogenerated Fenton's reagent. *Water Res.* **35**, 3987–3992 (2001).
4. Gogate, P. R. Hydrodynamic cavitation for food and water processing. *Food Bioprocess Technol.* **4**, 996–1011 (2011).
5. Kelkar, M. A., Gogate, P. R. & Pandit, A. B. Cavitation as a novel tool for process intensification of biodiesel synthesis. In *Proceedings 6th International Symposium on Catalysis in Multiphase Reactors* (Pune, India, 2007).
6. Gągol, M., Przyjazny, A. & Boczkaj, G. Highly effective degradation of selected groups of organic compounds by cavitation based AOPs under basic pH conditions. *Ultrason. Sonochem.* **45**, 257–266 (2018).
7. Boczkaj, G., Gągol, M., Klein, M. & Przyjazny, A. Effective method of treatment of effluents from production of bitumens under basic pH conditions using hydrodynamic cavitation aided by external oxidants. *Ultrason. Sonochem.* **40**, 969–979 (2018).
8. Bagal, M. V. & Gogate, P. R. Degradation of diclofenac sodium using combined processes based on hydrodynamic cavitation and heterogeneous photocatalysis. *Ultrason. Sonochem.* **21**, 1035–1043 (2014).
9. Thanekar, P., Garg, S. & Gogate, P. R. Hybrid treatment strategies based on hydrodynamic cavitation, advanced oxidation processes, and aerobic oxidation for efficient removal of naproxen. *Ind. Eng. Chem. Res.* **59**, 4058–4070 (2020).
10. Arany, E. et al. Degradation of naproxen by UV, VUV photolysis and their combination. *J. Hazard. Mater.* **262**, 151–157 (2013).
11. Kanakaraju, D., Motti, C. A., Glass, B. D. & Oelgemöller, M. TiO_2 photocatalysis of naproxen: effect of the water matrix, anions and diclofenac on degradation rates. *Chemosphere* **139**, 579–588 (2015).
12. Kim, I., Yamashita, N. & Tanaka, H. Performance of UV and UV/H_2O_2 processes for the removal of pharmaceuticals detected in secondary effluent of a sewage treatment plant in Japan. *J. Hazard. Mater.* **166**, 1134–1140 (2009).
13. Thanekar, P., Panda, M. & Gogate, P. R. Degradation of carbamazepine using hydrodynamic cavitation combined with advanced oxidation processes. *Ultrason. Sonochem.* **40**, 567–576 (2018).
14. Wang, M. *Advanced Yolk-Shell Nanoparticles as Nanoreactors for Catalysis*, *Department of Chemical Engineering.* Dissertation, Curtin University, USA, (2017).
15. Habibi Zare, M. & Mehrabani-Zeinabad, A. Rational design and synthesis of 3D nanoreactors for green fuel production: design band gap Y@DS photocatalyst under visible irradiation. *ACS Appl. Energy Mater.* **6**, 3173–3199 (2023).
16. Habibi Zare, M. & Mehrabani-Zeinabad, A. Yolk@Wrinkled-double shell smart nanoreactors: new platforms for mineralization of pharmaceutical wastewater. *Front. Chem*. **11**, 1211503 (2023).
17. Yuan, N., Gong, X., Sun, W. & Yu, C. Advanced applications of Zr-based MOFs in the removal of water pollutants. *Chemosphere* **267**, 128863 (2021).
18. Ahmadijokani, F. et al. Metal-organic frameworks and electrospinning: a happy marriage for wastewater treatment. *Adv. Funct. Mater.* **32**, 2207723 (2022).
19. Kaur, H. et al. Metal–organic framework-based materials for wastewater treatment: superior adsorbent materials for the removal of hazardous pollutants,. *ACS omega* **8**, 9004–9030 (2023).
20. Chen, Y. et al. Application of modified metal-organic frameworks in water treatment. *Mater. Today Chem.* **30**, 101577 (2023).
21. Shah, S. S. A. et al. Recent trends in wastewater treatment by using metal-organic frameworks (MOFs) and their composites: a critical view-point. *Chemosphere* **349**, 140729 (2024).
22. Lu, Y. et al. Recent advances in metal organic framework and cellulose nanomaterial composites. *Coord. Chem. Rev.* **461**, 214496 (2022).

23. Habibi Zare, M. & Mehrabani-Zeinabad, A. Yolk@ Wrinkled-double shell smart nanoreactors: new platforms for mineralization of pharmaceutical wastewater. *Front. Chem.* **11**, 1211503 (2023).
24. Habibi Zare, M. & Mehrabani-Zeinabad, A. Rational design and synthesis of 3D nanoreactors for green fuel production: design band gap Y@ DS photocatalyst under visible irradiation. *ACS Appl. Energy Mater.* **6**, 3173–3199 (2023).
25. Bagal, M. V. & Gogate, P. R. Wastewater treatment using hybrid treatment schemes based on cavitation and Fenton chemistry: a review. *Ultrason. Sonochem.* **21**, 1–14 (2014).
26. Rajoriya, S., Bargole, S. & Saharan, V. K. Degradation of reactive blue 13 using hydrodynamic cavitation: effect of geometrical parameters and different oxidizing additives. *Ultrason. Sonochem.* **37**, 192–202 (2017).
27. Kanthale, P. M., Gogate, P. R., Pandit, A. B. & Wilhelm, A. M. Dynamics of cavitational bubbles and design of a hydrodynamic cavitational reactor: cluster approach. *Ultrason. Sonochem.* **12**, 441–452 (2005).
28. Gogate, P. R. & Pandit, A. B. A review of imperative technologies for wastewater treatment I: oxidation technologies at ambient conditions. *Adv. Environ. Res.* **8**, 501–551 (2004).
29. Thanekar, P. & Gogate, P. Application of hydrodynamic cavitation reactors for treatment of wastewater containing organic pollutants: intensification using hybrid approaches. *Fluids* **3**, 98 (2018).
30. Saharan, V. K., Rizwani, M. A., Malani, A. A. & Pandit, A. B. Effect of geometry of hydrodynamically cavitating device on degradation of orange-G. *Ultrason. Sonochem.* **20**, 345–353 (2013).
31. Rajoriya, S., Bargole, S., George, S. & Saharan, V. K. Treatment of textile dyeing industry effluent using hydrodynamic cavitation in combination with advanced oxidation reagents. *J. Hazard. Mater.* **344**, 1109–1115 (2018).
32. Bhagat, M. N., Badve, M. P. & Pandit, A. B. Synergistic degradation of 4-nitrophenol using hydrodynamic cavitation in combination with hydrogen peroxide. *Int. J. Sustain. Water Environ. Syst.* **7**, 55–58 (2015).
33. Saharan, V. K., Badve, M. P. & Pandit, A. B. Degradation of Reactive Red 120 dye using hydrodynamic cavitation. *Chem. Eng. J.* **178**, 100–107 (2011).
34. Joshi, R. K. & Gogate, P. R. Degradation of dichlorvos using hydrodynamic cavitation based treatment strategies. *Ultrason. Sonochem.* **19**, 532–539 (2012).
35. Kumar, M. S., Sonawane, S. H. & Pandit, A. B. Degradation of methylene blue dye in aqueous solution using hydrodynamic cavitation based hybrid advanced oxidation processes. *Chem. Eng. Process. Process Intensif.* **122**, 288–295 (2017).
36. Jawale, R. H., Dapurkar, O. & Gogate, P. R. Treatment of atrazine containing wastewater using cavitation based hybrid treatment approaches. *Chem. Eng. Process. Process Intensif.* **130**, 275–283 (2018).
37. Barik, A. J. & Gogate, P. R. Degradation of 2, 4-dichlorophenol using combined approach based on ultrasound, ozone and catalyst. *Ultrason. Sonochem.* **36**, 517–526 (2017).
38. Jawale, R. H., Gogate, P. R. & Pandit, A. B. Treatment of cyanide containing wastewater using cavitation based approach. *Ultrason. Sonochem.* **21**, 1392–1399 (2014).
39. Wang, X., Jia, J. & Wang, Y. Combination of photocatalysis with hydrodynamic cavitation for degradation of tetracycline. *Chem. Eng. J.* **315**, 274–282 (2017).
40. Wang, B., Jiao, H., Su, H. & Wang, T. Degradation of pefloxacin by hybrid hydrodynamic cavitation with H2O2 and O3. *Chemosphere* **303**, 135299 (2022).
41. Yi, L. et al. Construction of Z-scheme (TiO2/Er3+: YAlO3)/NiFe2O4 photocatalyst composite for intensifying hydrodynamic cavitation degradation of oxytetracycline in aqueous solution. *Sep. Purif. Technol.* **293**, 121138 (2022).
42. Christopher, E. B. *Cavitation and Bubble Dynamics* (Oxford University Press, 1995).

Acknowledgements

The authors extend their appreciation to Taif University, Saudi Arabia, for supporting this work through project number (TU-DSPP-2024-61). The authors wish to thank the research council of the Isfahan University of Technology. This research was funded by Taif University, Saudi Arabia, Project No. (TU-DSPP-2024-61).

Author contributions

S.S.: Conceptualization, methodology, supervision, resources, reviewing and editing, original draft preparation. S.A.: Investigation, funding acquisition, methodology. M.A.K.: Resources, investigation, formal analysis, reviewing and editing. M.H.Z.: Conceptualization, methodology, experimental, resources, reviewing and editing, original draft preparation. A.M.-Z.: conceptualization, methodology, experimental, resources, supervision, reviewing and editing.

Competing interests

The authors declare no competing interests.

Additional information

Supplementary information The online version contains supplementary material available at https://doi.org/10.1038/s41545-024-00345-2.

Correspondence and requests for materials should be addressed to Saeed Shirazian.

Reprints and permissions information is available at http://www.nature.com/reprints

Publisher's note Springer Nature remains neutral with regard to jurisdictional claims in published maps and institutional affiliations.

[1]Institute of Research and Development, Duy Tan University, Da Nang, Vietnam. [2]School of Engineering & Technology, Duy Tan University, Da Nang, Vietnam. [3]Department of Pharmaceutics and Industrial Pharmacy, College of Pharmacy, Taif University, P.O. Box 11099 Taif 21944, Saudi Arabia. [4]Department of Chemistry, College of Science, U.A.E. University, Al-AinP.O. Box 17551UAE. [5]Department of Chemical Engineering, Isfahan University of Technology, 84156-83111 Isfahan, Iran. ✉e-mail: saeedshirazian@duytan.edu.vn